ADVANCED MATERIALS
www.advmat.de

Effect of an Ultrathin TiO_2 Layer Coated on Submicrometer-Sized ZnO Nanocrystallite Aggregates by Atomic Layer Deposition on the Performance of Dye-Sensitized Solar Cells

By *Kwangsuk Park, Qifeng Zhang, Betzaida Battalla Garcia, Xiaoyuan Zhou, Yoon-Ha Jeong,* and *Guozhong Cao**

Since the advent of dye-sensitized solar cells (DSCs), which have achieved ~11% of power conversion efficiency (PCE) in TiO_2-based photoelectrodes, a lot of efforts have been devoted to make low-cost, light-weight, high-performance photovoltaic devices.[1–3] Nanostructured metal oxides are one of key factors in determining the PCE of DSCs, because the nanostructured networks provide a huge surface area to accommodate a large quantity of dye molecules that relate to the light harvesting of a photoelectrode in DSCs.

ZnO is a good alternative of TiO_2 because it has a similar band gap but higher electron mobility than TiO_2.[4–7] The mobility of ZnO is about 115–155 $cm^2 V^{-1} s^{-1}$, much higher than that of TiO_2, ~10^{-5} $cm^2 V^{-1} s^{-1}$. Recently, DSCs with photoelectrodes made of submicrometer-sized aggregates of ZnO nanocrystallites demonstrated a PCE of 5.4% due to much enhanced light scattering without compromising the surface area for dye molecule adsorption.[8–10] A porous structured ZnO aggregates of nanocrystallites were thought to be helpful to retain their high surface area. Although this PCE is still lower than that of TiO_2 DSCs, it doubled the PCE of ZnO nanocrystallite DSCs.

Atomic layer deposition (ALD) has been used to introduce extremely thin and conformal coating due to its unique self-limiting nature and low growth temperature; lots of semiconductor materials like TiO_2, ZnO, SnO, and Al_2O_3 can be grown by ALD.[11–13] In this study, we utilized ALD to deposit ultrathin TiO_2 layer on the porous structure of ZnO aggregates and demonstrated much enhanced PCE of ZnO DSC with photoelectrodes made of submicrometer-sized aggregates of ZnO nanocrystallites.

As illustrated schematically in Figure 1a–c, TiO_2 ultrathin layer deposited by ALD would form a complete and conformal coverage on the surface and even inside pores of ZnO that would otherwise be exposed to dye electrolyte during the dye loading. Consequently, all the dye molecules would adsorb onto the surface of TiO_2 coating. Such an ultrathin and conformal ALD coating would not change the morphology the underline ZnO structures as shown in Figure 1e and 1f. The coating of TiO_2 layer on the surface of ZnO by ALD is presumably so thin that would not affect any detectable change in the morphology by means of scanning electron microscopy (SEM). Brunauer Emmett Teller (BET) results demonstrate that micropores inside each aggregate still remain after ALD, indicating that the porous structure of ZnO is preserved. As shown in Table 1, the slight decrease in the size and volume of the micropore was observed due to the introduction of ALD-TiO_2 layer. In addition, the connections between adjacent ZnO nanocrystallites would retain to ensure a favorable electron motion through ZnO (as suggested in Fig. 1d). Such structure would improve the surface stability with enhanced dye loading on the ZnO surface, while retains the advantage of high electron mobility in ZnO.

It is reported that the growth rate of TiO_2 at the substrate temperature of 200–250 °C ranges from 0.03 to 0.06 nm per one cycle so the thickness of TiO_2 grown by ALD for 10 cycles in the present investigation is estimated to be 0.3–0.6 nm.[14,15] X-ray diffraction (XRD) analysis did not reveal any diffraction peak associated with TiO_x including TiO_2, which corroborates with the fact that XRD is incapable of detecting an ultrathin layer of TiO_2.

It is not possible to tell if the ultrathin ALD-TiO_2 coating is of crystallites or amorphous, though the literature strongly suggests that it is crystallites, especially anatase phase when it is annealed above 400 °C.[15–17]

X-ray photoelectron spectroscopy (XPS) was carried out to verify the presence of ALD-TiO_2 coating on the surface of ZnO (see Fig. S1 in Supporting Information). Only a weak peak of Ti 2p with a binding energy of 459 eV was observed. Ti 2p spectrum could be resolved in three spin-orbit components with binding energies of 455.9, 456.7, and 458.5 eV and each of them corresponds to TiO, Ti_2O_3, and TiO_2 fractions, respectively.[18,19] The Ti 2p binding energy obtained in the current study is in a good agreement with that of Ti^{4+} which is 458.5 eV. Compositional analysis shows the content of Ti is 0.2–0.3 at %, consistent with the fact that the growth rate of TiO_2 by ALD is very slow, ~0.05 nm per cycle.[14,15]

Electrochemical impedance spectroscopy (EIS) analysis revealed appreciable difference in the charge transfer resistance

[*] Prof. G. Z. Cao, K. Park, Dr. Q. F. Zhang, B. B. Garcia, Dr. X. Y. Zhou
Department of Materials Science and Engineering, University of Washington
Seattle, WA (USA)
E-mail: gzcao@u.washington.edu
Prof. Y.-H. Jeong
National Center for Nanomaterials Technology
Postech, Pohang (Korea)

DOI: 10.1002/adma.200903219

© 2010 WILEY-VCH Verlag GmbH & Co. KGaA, Weinheim

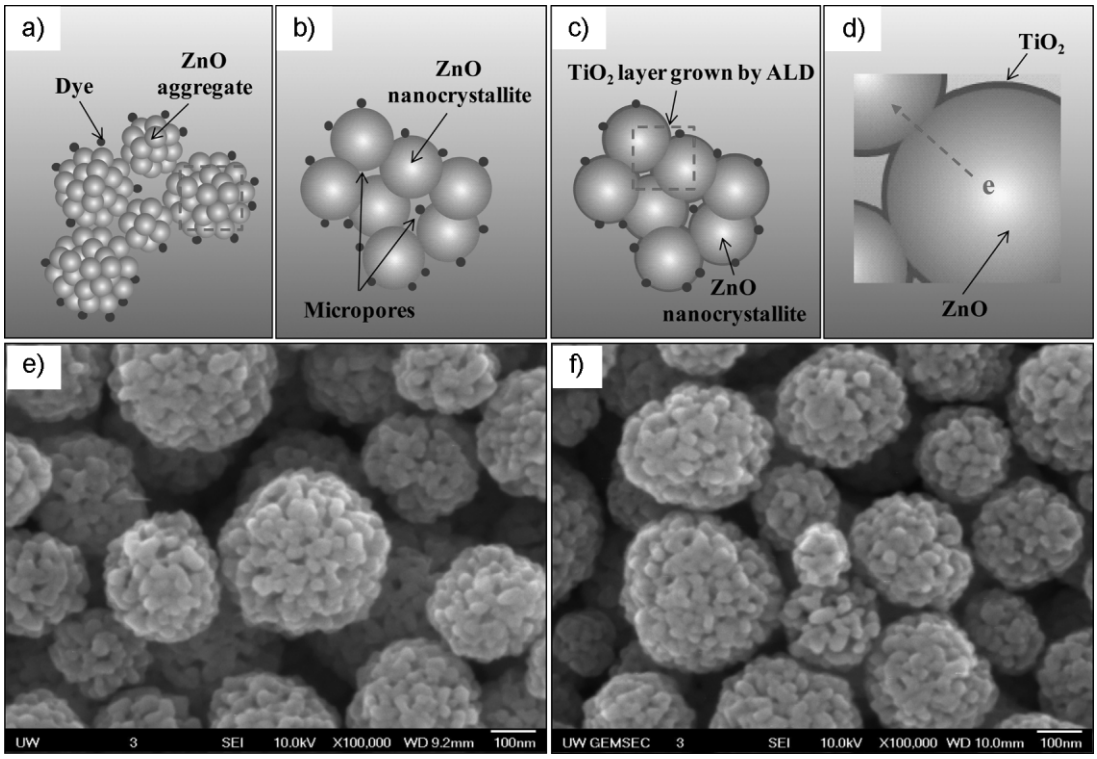

Figure 1. Schematics illustrating a) ZnO aggregates adsorbed with dye molecules, b) ZnO nanocrystallites containing micropores, c) conformal ALD-TiO_2 thin layer on the surface of ZnO nanocrystallites, d) enlarged schematic showing the details of conformal ALD-TiO_2 coating on ZnO surface and the uninterrupted connection between adjacent ZnO nanocrystallites for efficient electron motion, and SEM images of photoelectrode films of e) submicrometer-sized aggregates of ZnO nanocrystallites, and f) submicrometer-sized aggregates of ZnO nanocrystallites coated with thin TiO_2 layer.

at the aggregate/electrolyte interface in the ZnO films with and without ultrathin ALD-TiO_2 layer. Figure 2 shows the typical EIS Nyquist plots of ZnO film with and without TiO_2 coating; they all exhibit two semi-circles responding to different charge transfer mechanisms. The EIS Nyquist plot for DSCs would usually compose of three semi-circles but the EIS test in this study stopped after getting the second semicircle as this circle is directly related to the charge transfer at the aggregate/electrolyte interface where TiO_2 layer was introduced.[20,21] It is obvious that the charge transfer resistance assigned to the electron transfer at the aggregate/electrolyte interface (as denoted as R3 in Fig. 2) increased appreciably with the introduction of ALD-TiO_2 layer under otherwise the same conditions. Such a change is expected as the total resistance would be additive of the less conductive TiO_2 layer ($\sim 10^3$–$10^4\ \Omega$cm) and the more conductive ZnO core ($\sim 1\ \Omega$cm).[22–24] Such a change in the interface charge transfer resistance is a strong indication of the presence of thin TiO_2 coating on the surface of ZnO.

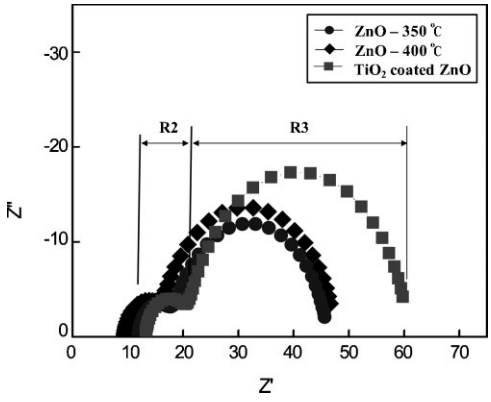

Figure 2. a) Nyquist plots of the ZnO films annealed at 350 and 400 °C and TiO_2 coated ZnO film annealed finally at 400 °C.

Table 1. BET data of micropores existing in the ZnO and TiO_2 coated ZnO aggregates.

	DA_{size} [nm] [a]	DA_{volume} [cc g^{-1}]	DR_{size} [nm] [b]	DR_{volume} [cc g^{-1}]
ZnO	2.08	0.041	1.775	0.026
TiO_2-coated ZnO	1.96	0.033	1.591	0.022

[a] Dubinin–Astakhov method. [b] Dubinin–Radushkevich method.

Solar cells with working electrodes consisting of the ZnO and TiO_2 coated ZnO films were tested under illumination with 100 mW cm^{-2} intensity. The responses of the solar cells to the illumination as a form of *J–V* curve are represented in Figure 3 and the performances of the solar cells such as open circuit voltage (V_{oc}), short circuit current density (J_{sc}), fill factor (FF), and overall conversion efficiency (η) can be calculated from the *J–V*

WILEY InterScience DISCOVER SOMETHING GREAT
© 2010 WILEY-VCH Verlag GmbH & Co. KGaA, Weinheim

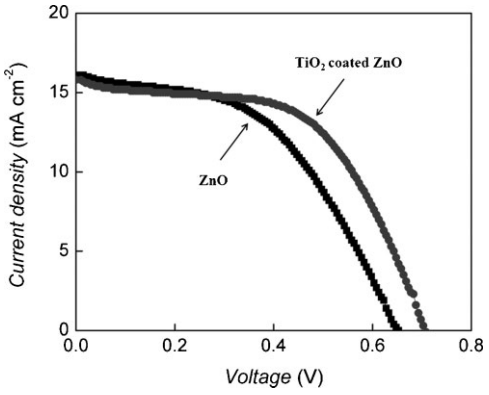

Figure 3. *J–V* curve of the solar cells with the electrodes composed of the ZnO and TiO_2 coated ZnO films under illumination with the power of 100 mW cm^{-2}.

curve through the relationships $\eta = J_{max}\ V_{max}/P_{in} \times 100$ and $FF = J_{max}\ V_{max}/J_{sc}\ V_{oc}$, where J_{max} and V_{max} are maximal photocurrent density and photovoltage in the *J–V* curve, respectively and P_{in} is the illumination power density. The results are summarized in Table 2.

While the overall PCE of 5.2% was achieved in ZnO-based solar cell, consistent with the result previously reported,[9] ZnO DSC with ALD-TiO_2 coating offered a higher PCE of 6.3% and an open circuit voltage of 709 mV. Although more research is needed to gain a better understanding of such a noticeable enhancement in both PCE and open circuit voltage with ALD-TiO_2 coating, a shell structure is often employed to suppress recombination which is considered as one of reasons for reducing open circuit voltage.[25,26] Although ZnO and TiO_2 have the same electronic structure, there is the concentration gradient of the electrons injected from the excited dye molecules between the ZnO core and TiO_2 shell due to their size difference; high electron concentration in ZnO and low electron concentration in TiO_2. In this kind of n–n^+ heterojunction at the ZnO/TiO_2 interface, a built-in potential is induced due to the electron concentration gradient, as shown:[27]

$$V_\phi = \frac{kT}{q} \ln \frac{N_d^+}{N_d} \quad (1)$$

Where V_ϕ is a potential gradient caused by the concentration gradient of electrons between the core and the shell, k the Boltzmann's constant, T the temperature, q the electron charge, and N_d^+ and N_d are the electron concentration in the ZnO core and the TiO_2 shell, respectively. The electric field generated by the potential gradient between the core and shell can confine the electrons in the ZnO core and eventually the recombination can be suppressed and a higher open circuit voltage is obtained. The suppressed recombination due to the presence of the TiO_2 shell also gives rise to an increase in an FF from 0.48 to 0.56.[28]

Table 2. Performances of the solar cells with the electrode made of ZnO and TiO_2 coated ZnO films.

	V_{oc} [V]	J_{sc} [mA cm^{-2}]	FF	η [%]
ZnO	0.658	16.3	0.48	5.2
TiO_2-coated ZnO	0.709	15.8	0.56	6.3

The change of the short circuit current density is a little complicated. However, there is no difference in J_{sc} between the ZnO and TiO_2 coated ZnO DSCs. Three factors are considered in determining the short circuit current density: (i) amount of dyes adsorbed onto the ZnO or TiO_2 surface for capturing the photons and generating electron–hole pairs, (ii) charge collection, and (iii) electron injection to semiconductors. It is obvious that the introduction of TiO_2 layer as a shell increased an efficiency of charge collection through suppressing recombination as revealed by EIS analysis.[25,29] In addition, the introduction of TiO_2 layer promotes dye adsorption; ~0.080 mg cm^{-2} dye adsorbed onto ALD-TiO_2 coated ZnO DSC as compared to ~0.076 mg cm^{-2} on ZnO DSC (see Fig. S3 in Supporting Information). More dyes favor photon-capturing and electron–hole generation and, thus, lead to higher short circuit current density. It would be expected that the J_{sc} is increased due to the effect of these two factors but the J_{sc} remained unchanged. The electron injection would become lower with the introduction of ALD-TiO_2 layer, which also would be a barrier layer to electrons that move from photoexited dye molecules to semiconductor, which was often observed in the core/shell structures.[25,26,30,31]

In conclusion, the submicrometer-sized aggregates of ZnO nanocrystallites were successfully coated with ultrathin TiO_2 layer by means of ALD to increase the PCE of DSCs. The ultrathin ALD-TiO_2 layer did not cause any perceivable change in the morphology and the micropore structure of ZnO aggregates. The introduction of the TiO_2 ultrathin layer results in more than 20% enhancement in the PCE from 5.2% to 6.3%. The ALD-TiO_2 layer increased both the open circuit voltage and the FF as a result of the suppressed surface charge recombination without impairing the photocurrent density.

Experimental

ZnO aggregates were synthesized through hydrolysis of 0.9855 g of zinc acetate dihydrate in 45 mL of diethylene glycol at 160 °C as reported previously [9]. The as-obtained ZnO aggregate colloidal solution was centrifuged at 6000 rpm for 25 min to separate the ZnO aggregates from the solvent. After removing the solvent, ethanol was applied to wash out the remaining aggregates, followed by sonication–centrifugation processes. The resultant ZnO aggregates were finally re-dispersed in 5 mL of ethanol to make a ZnO film. The ZnO film was fabricated on a FTO glass with an active area of 0.49 cm^2 by using a drop-cast method and annealed at 350 °C for 1 h to remove organic residues and improve a connection among the ZnO aggregates. The thickness of ZnO film was controlled to be about 10 μm.

Titanium isopropoxide [$Ti(OCH(CH_3)_2)_4$] and distilled water were used as a precursor and an oxidant, respectively to deposit TiO_2 on the surface of the ZnO aggregate for ALD. The temperatures were kept at 50 and 25 °C for the precursor and the oxidant, respectively and nitrogen gas was used as a carrier gas to deliver them more effectively. The substrate temperature was kept at 220 °C during the ALD process. One cycle is composed of (i) the precursor exposure (ii) purge the precursor (iii) the oxidant exposure, and (iv) purge the oxidant and totally 10 cycles were carried out to deposit an ultrathin TiO_2 layer. After ALD process, the TiO_2 coated ZnO film was

© 2010 WILEY-VCH Verlag GmbH & Co. KGaA, Weinheim

re-annealed at 400 °C for 1 h to get anatase TiO_2 as well as to remove any residue formed during ALD process.

The as-received ZnO and the TiO_2 coated ZnO films first were sensitized with 0.5 mM ruthenium complex *cis*-[$RuL_2(NCS)_2$] (commercially known as N3) in ethanol for 80 and 60 min, respectively. The electrolyte is composed of 0.6 M tetrabutylammonium iodide, 0.1 M lithium iodide, 0.1 M iodine, and 0.5 M 4-tert-butylpyridine in acetonitrile. The sensitized working electrode and the counter electrode of Pt-coated silicon were sandwitched.

SEM (JSM-7000) was used to study the morphology of the ZnO and TiO_2 coated ZnO aggregates. BET (NOVA 4200e) was carried out to measure the size of micropores in the ZnO aggregates. XPS was applied to detect ultrathin TiO_2 layer deposited on the ZnO aggregates by ALD. EIS was carried out through the Solartron 1287A coupling with the Solartron 1260 FRA/impedance analyzer. The applied ac amplitude and dc potential were 10 mV and −0.7 V, respectively. The solar cell performances were characterized using an HP 4155A programmable semiconductor parameter analyzer under AM 1.5 simulated sunlight with the power density of 100 mW cm^{-2}.

Acknowledgements

This work was supported financially in part by the U.S. Department of Energy, the office of Basic Energy Sciences, Division of Materials and Engineering under Award No. DE-FG02-07ER46467 (Q.F.Z.), National Science Foundation (DMI-0455994 and DMR-0605159), Air Force Office of Scientific Research (AFOSR-MURI, FA9550-06-1-0326), Pacific Northwest National Laboratories (PNNL), and National Center for Nanomaterials Technology (NCNT, Korea), Washington Research Foundation (WRF), the University of Washington (TGIF), and Intel Corporation. XPS analyses were carried out in the National ESCA and Surface Analysis Center for Biomedical Problems (EB-002027). B.B.G. acknowledges the NSF-16ERT fellowship (DGE-0654252). Supporting Information is available online from Wiley InterScience or from the authors.

Received: September 18, 2009
Revised: October 23, 2009
Published online: April 7, 2010

[1] B. O'Regan, M. Grätzel, *Nature* **1991**, *353*, 737.
[2] A. Hagfeldt, M. Grätzel, *Acc. Chem. Res.* **2000**, *33*, 269.
[3] M. Grätzel, *J. Photochem. Photobiol., A* **2004**, *164*, 3.
[4] M. Grätzel, *Nature* **2001**, *414*, 338.
[5] E. M. Kaidashew, M. Lorenz, H. von Wenckstern, A. Rahm, H. C. Semmelhack, K. H. Han, G. Benndorf, C. Bundesman, H. Hochmuth, M. Grundmann, *Appl. Phys. Lett.* **2003**, *82*, 3901.
[6] Th. Dittrich, E. Lebedev, J. Weidmann, *Phys. Status Solidi A* **1998**, *165*, R5.
[7] Q. F. Zhang, C. S. Dandeneau, X. Y. Zhou, G. Z. Cao, *Adv. Mater.* **2009**, *21*, 1.
[8] T. P. Chou, Q. F. Zhang, G. E. Fryxell, G. Z. Cao, *Adv. Mater.* **2007**, *19*, 2588.
[9] Q. F. Zhang, T. P. Chou, B. Russo, S. A. Jenekhe, G. Z. Cao, *Angew. Chem, Int. Ed.* **2008**, *47*, 2402.
[10] Q. F. Zhang, T. P. Chou, B. Russo, S. A. Jenekhe, G. Z. Cao, *Adv. Funct. Mater.* **2008**, *18*, 1654.
[11] S. M. Rossnagel, H. Kim, *Proc. of the IEEE 2001 Intl. Interconnect Tech. Conf.* **2001**, Burlingame, CA, p. 3.
[12] M. Knez, K. Nielsch, L. Niinisto, *Adv. Mater.* **2007**, *19*, 3425.
[13] A. Rosental, A. Tarre, A. Geast, T. Uustare, V. Sammelsely, *Sens. Actuators, B* **2001**, *77*, 297.
[14] J. Aarik, A. Aidla, T. Uustare, M. Ritala, M. Leskela, *Appl. Surf. Sci.* **2000**, *161*, 385.
[15] T. W. Hamann, A. B. F. Martinson, J. W. Elam, M. J. Pellin, J. T. Hupp, *J. Phys. Chem. C* **2008**, *112*, 10303.
[16] M. Pal, J. G. Serrano, P. Santiago, U. Pal, *J. Phys. Chem. C* **2007**, *111*, 96.
[17] M. Ritala, M. Leskelä, *Chem. Mater.* **1993**, *5*, 1174.
[18] P. M. Kumar, S. Badrinarayanan, M. Sastry, *Thin Solid Films* **2000**, *358*, 122.
[19] S.-J. Roh, R. S. Mane, S.-K. Min, W.-J. Lee, C. D. Lokhande, S.-H. Han, *Appl. Phys. Lett.* **2006**, *89*, 253512.
[20] Q. Wang, J. E. Moser, M. Grätzel, *J. Phys. Chem. B* **2005**, *109*, 14945.
[21] F. F. Santiago, J. Biquert, G. G. Belmonte, G. Boschloo, A. Hagfeldt, *Sol. Energy Mater. Sol. Cells* **2005**, *87*, 117.
[22] M. Law, L. E. Greene, A. Radenovie, T. Kuykendall, J. Liphardt, P. Yang, *J. Phys. Chem. B* **2006**, *110*, 22652.
[23] M. Law, L. E. Greene, J. C. Johnson, R. Saykally, P. Yang, *Nat. Mater.* **2005**, *4*, 455.
[24] D. Chen, Y. Gao, G. Wang, H. Zhang, W. Lu, J. Li, *J. Phys. Chem. C* **2007**, *111*, 13163.
[25] Y. Diamant, S. Chappel, S. G. Chen, O. Melamed, A. Zaban, *Coord. Chem. Rev.* **2004**, *248*, 1271.
[26] K. M. P. Bandaranayake, M. K. I. Senevirathna, P. M. G. M. P. Weligamuwa, K. Tennakone, *Coord. Chem. Rev.* **2004**, *248*, 1277.
[27] O. V. Roos, *J. Appl. Phys.* **1978**, *49*, 3503.
[28] N. Koide, A. Islam, Y. Chiba, L. Han, *J. Photochem. Photobiol., A* **2006**, *182*, 296.
[29] V. Thavasi, V. Renugopalakrishnan, R. Jose, S. Ramakrishna, *Mater. Sci. Eng, R* **2009**, *63*, 81.
[30] T. W. Hamann, O. K. Farha, J. T. Hupp, *J. Phys. Chem. C* **2008**, *112*, 19756.
[31] Y. Diamant, S. G. Chen, O. Melamed, A. Zaban, *J. Phys. Chem. B* **2003**, *107*, 1977.

WILEY InterScience® DISCOVER SOMETHING GREAT
© 2010 WILEY-VCH Verlag GmbH & Co. KGaA, Weinheim